Silicon (2021) 13:573–585
https://doi.org/10.1007/s12633-020-00451-z

ORIGINAL PAPER

Photo-Thermoelastic Model with Time-Fractional of Higher Order and Phase Lags for a Semiconductor Rotating Materials

Kadry Zakaria[1] · Magdy A. Sirwah[1] · Ahmed E. Abouelregal[2,3] · Ali F. Rashid[1]

Received: 4 December 2019 / Accepted: 11 March 2020 / Published online: 31 March 2020

Abstract

In this work, a modified generalized fractional photothermeolastic model is constructed on the basis of the fractional calculus technique. For the considered model, Fourier law is introduced using the Taylor series expansion of higher time-fractional. The formulated model is an extension to the thermoelastic theories proposed by Lord–Shulman Lord and Shulman (J. Mech. Phys. Solid 15:299-309, 1967). Tzou (J Heat Transfer 117: 8-16, 1995) and fractional thermoelastic model introduced by Ezzat (Applied Mathematical Modelling 35:4965-4978, 2011). The model is then implemented to investigate photothermoelastic interaction in a rotating semiconductor half-space stressed by magnetic field. The numerical results of the effects of some physical functions are illustrated graphically to estimate the influences of the fractional parameter, the rotation parameter, and the higher-order time-fractional. It is shown that these parameters have a required significant influence on the physical fields.

Keywords Photo-thermoelasticity · Time-fractional · Higher-order · Rotation · Plasma-elastic wave

Nomenclature

λ, μ	Lame's constants
α_t	thermal expansion coefficient
C_e	specific heat
$\gamma = (3\lambda + 2\mu)\alpha_t$	thermal coupling parameter
T_0	environmental temperature
$\theta = T - T_0$	temperature increment
T	absolute temperature
u	displacement vector
$e = div\ u$	cubical dilatation
σ_{ij}	stress tensor
e_{ij}	strain tensor
q	heat flux vector
n_0	equilibrium carrier concentration
$\overrightarrow{H}$	magnetic field
$\overline{h}$	induced magnetic field
$d_n = (3\lambda + 2\mu)\delta_n$	diffusion coupling parameter
Ω	angular velocity vector
a	wave number in the direction
h	coefficient of the surface heat transfer
K	thermal conductivity
ρ	material density
Q	heat source
t	the time
δ_{ij}	Kronecker's delta function
τ	minority carrier lifetime
τ_q	phase lag of heat flux
τ_θ	phase lag of temperature
E_g	semiconducting energy gap
δ_n	electronic deformation coefficient
D_E	diffusion coefficient
N	carrier density
κ	thermal activation coupling parameter
$\overrightarrow{E}$	induced electric field
$\overrightarrow{J}$	current density

✉ Ahmed E. Abouelregal
ahabogal@mans.edu.eg; ahabogal@gmail.com

Kadry Zakaria
kadry.zakaria@science.tanta.edu.eg

Magdy A. Sirwah
Magdy.sirwah@science.tanta.edu.eg

Ali F. Rashid
PG_21166@science.tanta.edu.eg; a_f_rashid@yahoo.com

[1] Mathematics Department, Faculty of Science, Tanta University, Tanta, Egypt

[2] Mathematics Department, Faculty of Science, Mansoura University, Mansoura 35516, Egypt

[3] Mathematics Department, College of Science and Arts, University of Aljouf, Al-Qurayat, Saudi Arabia

μ_0	magnetic permeability
τ_1	lifetime of photogenerated electron
ε_0	electric permeability

1 Introduction

The branch of fractional calculus was utilized to investigate different current types for the materials physical properties. Fractional derivatives and integrals theory was originally founded in nineteenth century's second half. The most significant improvement by using the usage of fractional differential equations in several enforcement is their nonlocal property.

Fractional calculus theories have been applied in numerous fields; chemistry, statistic physics, economics and biological sciences [1–3]. The history and classical conversion rules on this topic were well discussed in the conducted materials by Podlubny [4]. Recently, the field of fractional calculus was applied in the thermoelasticity field. Povstenko [5] constructed a new thermoelastic fractional order model based on Caputo fractional derivative [6]. Youssef [7] and Sherief et al. [8] have introduced another some models about generalized thermoelasticity which constructed on fractional time derivatives.

Abouelregal [9] applied the fractional order thermoe lasticity model to studied thermoelastic influences on a semi-infinite piezoelectric solid. Abouelregal and Zenkour [10] discussed the influence of the model of fractional thermoelasticity on a rotating fiber-reinforced thermoelastic solid. Also, in [11] Abouelregal investigated the heat conduction equation with fractional order in an infinitely solid cylinder. In addition Zenkour and Abouelregal [12] considered the influence of the state-space approach two-temperature, and fractional order heat conduction on an unbounded body has a spherical cavity.

The classical thermoelastic theory depends on Fourier's law which forecasts an unlimited velocity of heat propagation. With a specific end goal to wipe out this paradox of unlimited speed of the thermal waves, a modified model for thermoelastic theory which is in a hyperbolic type was introduced by Lord and Shulman [13]. The thermoelasticity theory without energy dissipation is an alternative model which is expressed by Green and Naghdi [14].

Investigation of thermoelastic plane wave in a nonrotating bodies is accepting significant attention in later years. Since most huge bodies in the universe and in our solar system like the moon, Earth and some planets have an angular velocity, it seems to be more reasonable to discuss the spread of thermoelastic and plane waves in the case of a rotating body. The influence of rotation on thermal waves is previously considered by several authors [15–19].

Photothermal spectroscopy is a set of great sensitivity procedures applied to calculate the thermal characteristics and optical absorption of a specimen. The photothermal spectroscopy foundation is a photo-generated variation in the thermal condition of the specimen. There are many utilizations of photothermal techniques for material and chemical analysis. Tam [20–22] is maybe first responsible for classifying through the great measure of writing and indicating the purpose of these techniques. A considerable lot of these applications are canvassed in a book proposed by Sell [23]. Spectroscopy is the science offered to the analysis of the interaction of the energy with the matter. The most established orderly technique of the effect of photothermal is accepted to be the correspondence gadget, the photophone, developed by Bell [24, 25]. He remarked that noticeable sound may be heard arriving from the tube fulfilled with different materials when the light bright on the diaphanous tube was modified. The sound was noisy when the tube was fulfilled with radiation assimilating solids or gases, and feeble when loaded with a liquid. The operational standards are currently well understood.

Viengerov [26] utilized the effect of photoacoustic to consider light assimilation in gases and attained an approximations of the concentration in the gas blends depend on the signal amounts. Rosencwaig et al. [27] displayed an examination on the deformations which happen at the surface of sample owing to the excitation by an engaged test beam. Under the thermoelasticity theory, Song et al. [28–30] presented the deflection of the semiconducting cantilevers due to the thermal optical excitation. Problems regarding generalized thermoelasticity models with dual phase lags have been discussed with many authors [31–36]. Abouelregal introduced a new modified model for photo-thermoelasticity with regard to a new consideration of generalized heat conduction equations with time-fractional order [37].

Recently, Chirita and Zampoli [38] investigated the thermoelastic model that describes the authentic coupling between the ultrafast deformation and the high-order lagging behavior. They considered that the interaction within numerous energy carriers as a direct consequence. Also, Chirita [39] took into account class of constitutive equations of the heat flux which describes the high-order influences in any lagging behavior of heat transportation.

Abouelregal [40] introduced a generalized thermoelastic modified model including multi-phase times and fractional order. He modified Green and Lindsay [41] heat conduction with two relaxation times and constitutive equations based on the Riemann–Liouville fractional integral operators. Also, Abouelregal [42] constructed a novel thermoelasticity heat conductivity higher order time-derivatives model by taking into consideration the theory of two-temperature including phase-lags. He used fading memory theory to restructure his proposed model. Abouelregal [43] modified the heat conduction using Taylor series expansion for time derivative in Green and Naghdi model without energy dissipation. Ramon Quintanilla [44] discussed the theory of two temperature thermoelasticity higher-order corresponding to Taylor expansions of higher order. Majchrzak [45] supplemented the DPL equation of second order derivative with respect to time and mixed higher order derivative with respect to both time and space by the adequate initial and boundary conditions. Rukolaine [46] studied the initial value problems for equations, for two models of heat conduction, depending on higher-order approximations to the constitutive relation of the dual-phase-lag.

In the current work, a generalized model of higher fractional order of time differential magneto-photo-thermoelasticity has been introduced in the presence of model of heat conduction with non-integer order derivative (fractional derivatives), where a rotating isotropic semiconductor medium subjected to a magnetic field. The solutions for the temperature, displacements and thermal stresses are obtained by using the normal mode method and have been illustrated graphically. In addition, the influence of the fractional parameter, rotation and magnetic field on the physical variables are numerically discussed and illustrated graphically.

2 Statement of the Problem

2.1 Basic Equations

The classical theory of heat conduction is based on Fourier's law; in which represent the relation between the heat flux vector $\boldsymbol{q}$ at a point x to the temperature gradient at the same point.

The equation of heat conduction is given by:

$$\boldsymbol{q}(\boldsymbol{x},t)=-K\nabla\theta(\boldsymbol{x},t) \tag{1}$$

The energy balance equation is given by

$$\rho C_e\frac{\partial\theta}{\partial t}+\gamma T_0\frac{\partial}{\partial t}(\mathrm{div}u)=-\mathrm{div}q+\rho Q \tag{2}$$

The DPL model which introduced by Tzou [47, 48] describes the process of thermal relaxation and thermalization behaviors that are interwoven in the ultrafast process of transportation of the heat in the electron gas. Two authentic relaxation times, named phase-lags symbolized by τ_θ and τ_q. In this model, the old Fourier's law (1) is changed to a general relation between heat flux vector $\boldsymbol{q}$ at a point x of the material at time $t+\tau_q$ and temperature gradient $\nabla\theta$ at the same point at time $t+\tau_\theta$ to be:

$$\boldsymbol{q}\left(\boldsymbol{x},t+\tau_q\right)=-K\nabla\theta(\boldsymbol{x},t+\tau_\theta) \tag{3}$$

The continuous functions $q(x,t+\tau_q)$ and $\nabla\theta(x,t+\tau_\theta)$ are considered fractional derivatives of order $k\alpha$, for any integer k where $k>1$ and for any α where $0<\alpha\le 1$. Using the expansion of Taylor series of time-fractional order provided by Jumarie [49] to the previous functions, yields:

$$\begin{aligned}\boldsymbol{q}\left(\boldsymbol{x},t+\tau_q\right)&=\sum_{k=0}^{\infty}\frac{\left(\tau_q\right)^{k\alpha}}{\Gamma(1+k\alpha)}\boldsymbol{q}^{(k\alpha)}\\ \nabla\theta(\boldsymbol{x},t+\tau_\theta)&=\sum_{k=0}^{\infty}\frac{\left(\tau_\theta\right)^{k\alpha}}{\Gamma(1+k\alpha)}\nabla\theta^{(k\alpha)}\end{aligned} \tag{4}$$

where $f^{(k\alpha)}$ is the time derivative of order $k\alpha$ of $f(t)$ and $\Gamma(1+k\alpha)=(k\alpha)!$ In the previous Eq. (4), we took into consideration the Riemann-Liouville fractional integral, this Riemann-Liouville formula was proposed as a generalization for the convolution integration type [1, 3–6, 50, 51]:

$$I^\alpha f(t)=\int_0^t\frac{(t-\tau)^{\alpha-1}}{\Gamma(\alpha)}f(\tau)d\tau \tag{5}$$

where I^α is the integral operator of Riemann–Liouville of order α, $f(t)$ is a Lebesgue integrable function. In case of $f(t)$ is perfectly continuous, then:

$$\lim_{\alpha\to 1}\left(\frac{d^\alpha}{dt^\alpha}f(t)\right)=f'(t) \tag{6}$$

Using Eq. (4) and retaining terms up to the order $(m\alpha)$ in τ_q and $(p\alpha)$ in τ_θ, Eq. (3) can be formulated in the shape:

$$\begin{aligned}&\left(1+\sum_{k=1}^{m}\frac{\left(\tau_q\right)^{k\alpha}}{(k\alpha)!}\frac{\partial^{k\alpha}}{\partial t^{k\alpha}}\right)\boldsymbol{q}\\ &=-K\left(1+\sum_{k=1}^{p}\frac{\left(\tau_\theta\right)^{k\alpha}}{(k\alpha)!}\frac{\partial^{k\alpha}}{\partial t^{k\alpha}}\right)\nabla\theta\end{aligned} \tag{7}$$

Eliminating $\boldsymbol{q}$ from Eqs. (2) and (7) leads to a modification form for the equation of heat transfer with higher fractional derivatives of time and two phase-lags, in the form:

$$\begin{aligned}&\left(1+\sum_{k=1}^{m}\frac{\left(\tau_q\right)^{k\alpha}}{(k\alpha)!}\frac{\partial^{k\alpha}}{\partial t^{k\alpha}}\right)\left[\rho C_e\frac{\partial\theta}{\partial t}+\gamma T_0\frac{\partial}{\partial t}(\mathrm{div}u)-\rho Q\right]\\ &=K\left(1+\sum_{k=1}^{p}\frac{\left(\tau_\theta\right)^{k\alpha}}{(k\alpha)!}\frac{\partial^{k\alpha}}{\partial t^{k\alpha}}\right)\nabla^2\theta\end{aligned} \tag{8}$$

From thermomechanical and mathematical points of view, the spatial behavior of the field solutions inside the lagging behavior framework was an important issue to be studied by many researchers [50–54]. However, they have taken into consideration equations only up to second order with respect to the time, and neglecting the higher-order effects of the thermal relaxing.

Equation (8) introduces a general model of fractional heat conduction of higher time-fractional order and two phase lags for an isotropic and a homogeneous rotating semiconductor material and below are additional governing equations for this model [45]:

Between strain and stress, the relations be:

$$\sigma_{ij} = 2\mu e_{ij} + \delta_{ij}\left[\lambda e_{ij} - \gamma\theta - d_n N\right] \tag{9}$$

The relation between the strain and displacement

$$2e_{ij} = u_{j,i} + u_{i,j} \tag{10}$$

The equation of motion

$$\mu u_{i,jj} + (\lambda + \mu)u_{j,ij} - \gamma\theta_{,i} - d_n N_{,i} + F_i = \rho \ddot{u}_i + \rho\left(\boldsymbol{\Omega} \times (\boldsymbol{\Omega} \times \boldsymbol{u}) + \left(2\boldsymbol{\Omega} \times \dot{\boldsymbol{u}}\right)\right)_i \tag{11}$$

The coupled plasma wave equation [28–30]:

$$D_E \nabla^2 N = \rho \frac{\partial N}{\partial t} + \frac{1}{\tau} N + \chi\theta + G \tag{12}$$

The induced electric field $\boldsymbol{E}$ and magnetic field $\boldsymbol{h}$ are due to the applied magnetic field $\boldsymbol{H}$, The Maxwell's equations of electromagnetic field, with charge density neglecting were written as:

$$\boldsymbol{J} = \nabla \times \boldsymbol{h} - \varepsilon_0 \frac{\partial \boldsymbol{E}}{\partial t}, \quad \nabla \times \boldsymbol{E} = -\mu_0 \frac{\partial \boldsymbol{h}}{\partial t}, \quad \boldsymbol{E} = -\mu_0\left(\frac{\partial \boldsymbol{u}}{\partial t} \times \boldsymbol{H}\right), \ \nabla \cdot \boldsymbol{h} = 0 \tag{13}$$

The Maxwell's equation for stresses is taken the form:

$$\tau_{ij} = \mu_0\left[H_i h_j + H_j h_i - H_k h_k \delta_{ij}\right] \tag{14}$$

For a perfect conductor, the Lorentz force $\boldsymbol{F}$ induced from the magnetic field $\boldsymbol{H}$ is:

$$\boldsymbol{F} = \mu_0(\nabla \times \boldsymbol{H}) \tag{15}$$

2.2 Derivation of the Problem Equations'

We will take in our consideration an isotropic and homogeneous semiconductor photo-thermoelastic solid with rectangular coordinate system (x, y, z). The semiconductor medium is rotating with a regular angular velocity $\boldsymbol{\Omega} = (0, \Omega, 0)$ about y-axis and under constant primary uniform magnetic field $\boldsymbol{H_0}$.

The displacement components of a 2-D problem have the forms

$$\boldsymbol{u}(x, z, t) \equiv (u, 0, w) \tag{16}$$

The cubical dilatation given by

$$e = \mathrm{div}(\boldsymbol{u}) = \frac{\partial u}{\partial x} + \frac{\partial w}{\partial z} \tag{17}$$

After applying the initial magnetic field $\boldsymbol{H_0}$, the components of Lorentz force are:

$$F_x = \mu_0 H_0^2\left(\frac{\partial^2 u}{\partial x^2} + \frac{\partial^2 w}{\partial x \partial z} - \mu_0\varepsilon_0 \frac{\partial^2 u}{\partial t^2}\right), \quad F_z = \mu_0 H_0^2\left(\frac{\partial^2 w}{\partial z^2} + \frac{\partial^2 u}{\partial x \partial z} - \mu_0\varepsilon_0 \frac{\partial^2 w}{\partial t^2}\right) \tag{18}$$

The equations of motion along x and z directions considering the Lorentz force takes the forms:

$$\left(\lambda + \mu + \mu_0 H_0^2\right)\frac{\partial e}{\partial x} + \mu\nabla^2 \mathrm{u} - \gamma\frac{\partial \theta}{\partial x} - d_n \frac{\partial N}{\partial x} = \left(\rho + \varepsilon_0\mu_0^2 H_0^2\right)\frac{\partial^2 \mathrm{u}}{\partial t^2} - \rho\Omega^2 u + 2\rho\Omega\frac{\partial w}{\partial t} \tag{19}$$

$$\left(\lambda + \mu + \mu_0 H_0^2\right)\frac{\partial e}{\partial z} + \mu\nabla^2 \mathrm{w} - \gamma\frac{\partial \theta}{\partial z} - d_n \frac{\partial N}{\partial z} = \left(\rho + \varepsilon_0\mu_0^2 H_0^2\right)\frac{\partial^2 \mathrm{w}}{\partial t^2} - \rho\Omega^2 u - 2\rho\Omega\frac{\partial u}{\partial t} \tag{20}$$

The generalized heat conduction equation with fractional order (8) in the absence of heat sources takes the following form:

$$K\left(1 + \sum_{k=1}^{p} \frac{\tau_\theta^{(K\alpha)}}{(K\alpha)!}\frac{\partial^{K\alpha}}{\partial t^{K\alpha}}\right)\left(\frac{\partial^2 \theta}{\partial x^2} + \frac{\partial^2 \theta}{\partial z^2}\right) = \left(1 + \sum_{k=1}^{m} \frac{\tau_q^{(K\alpha)}}{(K\alpha)!}\frac{\partial^{K\alpha}}{\partial t^{K\alpha}}\right)\left[\rho C_E \frac{\partial \theta}{\partial t} + \gamma T_0 \frac{\partial e}{\partial t} - \frac{E_g}{\tau} N\right] \tag{21}$$

Also, the constitutive Eqs. (9) may be reduced to

$$\begin{aligned} \sigma_{xx} &= (\lambda + 2\mu)\frac{\partial u}{\partial x} + \lambda\frac{\partial w}{\partial z} - \gamma\theta - d_n N \\ \sigma_{zz} &= (\lambda + 2\mu)\frac{\partial w}{\partial z} + \lambda\frac{\partial u}{\partial x} - \gamma\theta - d_n N \\ \sigma_{xz} &= \mu\left(\frac{\partial u}{\partial z} + \frac{\partial w}{\partial \mathrm{x}}\right) \end{aligned} \tag{22}$$

In addition, the coupled plasma Eq. (12) in x-z plane will be:

$$D_E\left(\frac{\partial^2 N}{\partial x^2} + \frac{\partial^2 N}{\partial z^2}\right) = \rho\frac{\partial N}{\partial t} + \frac{1}{\tau}N + \chi\theta \tag{23}$$

Now, let us introduce a decomposition form of the displacement vector:

$$\boldsymbol{u} = \nabla\Phi + \mathrm{curl}(\Psi) \tag{24}$$

From (19), the scalar potentials displacement Φ and Ψ which are associated with displacement components u and w as,

$$u=\frac{\partial\Phi}{\partial x}-\frac{\partial\Psi}{\partial z},\qquad w=\frac{\partial\Phi}{\partial z}+\frac{\partial\Psi}{\partial x}\tag{25}$$

From the displacement representation (25), we can get

$$\left(c_0^2\nabla^2+\Omega^2-\left(1+\varepsilon_0\mu_0a_0^2\right)\frac{\partial^2}{\partial t^2}\right)\Phi=\frac{1}{\rho}\left(\gamma\theta+d_nN+2\Omega\frac{\partial\Psi}{\partial t}\right)\tag{26}$$

$$\left(c_3^2\nabla^2+\Omega^2-\left(1+\varepsilon_0\mu_0a_0^2\right)\frac{\partial^2}{\partial t^2}\right)\Psi=2\Omega\frac{\partial\Phi}{\partial t}\tag{27}$$

$$\left(1+\sum_{k=1}^{m}\frac{\tau_q^{(K\alpha)}}{(K\alpha)!}\frac{\partial^{K\alpha}}{\partial t^{K\alpha}}\right)\left[\rho C_E\frac{\partial\theta}{\partial t}+\gamma T_0\frac{\partial}{\partial t}\left(\nabla^2\Phi\right)-\frac{E_g}{\tau}N\right]=K\left(1+\sum_{k=1}^{p}\frac{\tau_\theta^{(K\alpha)}}{(K\alpha)!}\frac{\partial^{K\alpha}}{\partial t^{K\alpha}}\right)\left(\frac{\partial^2\theta}{\partial x^2}+\frac{\partial^2\theta}{\partial z^2}\right)\tag{28}$$

Where

$$c_0^2=c_1^2+a_0^2,c_3^2=c_2^2+a_0^2,\quad c_1^2=\frac{\lambda+2\mu}{\rho},\quad a_0^2=\frac{\mu_0H_0^2}{\rho},\qquad c_2^2=\frac{\mu}{\rho}.\tag{29}$$

Using Eq. (25), the stresses can be written as

$$\begin{aligned}\sigma_{xx}&=\lambda\nabla^2\Phi+2\mu\frac{\partial}{\partial x}\left(\frac{\partial\Phi}{\partial x}-\frac{\partial\Psi}{\partial z}\right)-\gamma\theta-d_nN\\ \sigma_{zz}&=\lambda\nabla^2\Phi+2\mu\frac{\partial}{\partial z}\left(\frac{\partial\Psi}{\partial x}+\frac{\partial\Phi}{\partial z}\right)-\gamma\theta-d_nN\\ \sigma_{xz}&=2\mu\frac{\partial^2\Phi}{\partial x\partial z}+\mu\left(\frac{\partial^2\Psi}{\partial x^2}-\frac{\partial^2\Phi}{\partial z^2}\right)\end{aligned}\tag{30}$$

It is appropriate to introduce the following dimensionless quantities which defined as:

$$\left\{x',z',u',w'\right\}=\frac{\eta_0}{c_0}\{x,z,u,w\},\quad t'=\eta_0t,\quad\left\{\theta',N'\right\}=\frac{1}{\rho c_0^2}\{\gamma\theta,d_nN\},$$
$$\left\{\Phi',\Psi'\right\}=\frac{\eta_0^2}{c_0^2}\{\Phi,\Psi\},\quad\Omega'=\frac{\Omega}{\eta_0},\qquad\sigma_{ij}'=\frac{\sigma_{ij}}{\gamma T_0},\quad\eta_0=\frac{\rho C_Ec_0^2}{K}.\tag{31}$$

The basic governing equations after using the non-dimensional quantities (31) and suppressing the primes reduce to

$$\left(\nabla^2+\Omega^2-\left(1+\varepsilon_0\mu_0a_0^2\right)\frac{\partial^2}{\partial t^2}\right)\Phi=\theta+N+2\Omega\frac{\partial\Psi}{\partial t}\tag{32}$$

$$\left(c_3^2\nabla^2+c_0^2\Omega^2-c_0^2\left(1+\varepsilon_0\mu_0a_0^2\right)\frac{\partial^2}{\partial t^2}\right)\Psi=2c_0^2\Omega\frac{\partial\Phi}{\partial t}\tag{33}$$

$$\left(1+\sum_{k=1}^{p}\frac{\tau_\theta^{(K\alpha)}}{(K\alpha)!}\frac{\partial^{K\alpha}}{\partial t^{K\alpha}}\right)\left(\frac{\partial^2\theta}{\partial x^2}+\frac{\partial^2\theta}{\partial z^2}\right)=\left(1+\sum_{k=1}^{m}\frac{\tau_q^{(K\alpha)}}{(K\alpha)!}\frac{\partial^{K\alpha}}{\partial t^{K\alpha}}\right)\left[\frac{\partial\theta}{\partial t}+\varepsilon_1\frac{\partial}{\partial t}\left(\nabla^2\Phi\right)-\varepsilon_2N\right]\tag{34}$$

$$\nabla^2N=g_1\frac{\partial N}{\partial t}+g_2N+g_3\theta\tag{35}$$

Where

$$\varepsilon_1=\frac{\gamma^2T_0}{\rho^2c_0^2C_E},\quad\varepsilon_2=\frac{\gamma E_g}{\rho C_E\tau d_n},\quad g_1=\frac{\rho c_0^2}{D_E\eta_0},\quad g_2=\frac{c_0^2}{D_E\eta_0\tau},\quad g_3=\frac{\kappa d_nc_0^2}{D_E\eta_0^2}.\tag{36}$$

Substitute from Eq. (31), we get the stresses σ_{xx} and σ_{zz} as

$$\begin{aligned}\sigma_{xx}&=\frac{\partial u}{\partial x}+C_{12}\frac{\partial w}{\partial x}-\theta-N,\quad C_{12}=\frac{\lambda}{\lambda+2\mu}\\ \sigma_{zz}&=\frac{\partial w}{\partial z}+C_{12}\frac{\partial u}{\partial x}-\theta-N,\quad C_{13}=\frac{\mu}{\lambda+2\mu}\\ \sigma_{xz}&=C_{13}\left(\frac{\partial u}{\partial z}+\frac{\partial w}{\partial x}\right)\end{aligned}\tag{37}$$

3 The Problem Solution

The solution of the field quantities can be obtained by applying the technique of normal mode analysis, defined by:

$$\left\{u,w,\theta,\Phi,\Psi,N,\sigma_{ij}\right\}(x,z,t)=\left\{u^*,w^*,\theta^*,\Phi^*,\Psi^*,N^*,\sigma_{ij}^*\right\}(x)e^{\omega t+iaz}\tag{38}$$

where $\boldsymbol{\omega}$ is constant indicates (complex) frequency, $\boldsymbol{i}=\sqrt{-1}$, and $\boldsymbol{u^*}(\boldsymbol{x})$, $\boldsymbol{w^*}(\boldsymbol{x})$, $\boldsymbol{\theta^*}(\boldsymbol{x})$, $\boldsymbol{\Phi^*}(\boldsymbol{x})$, $\boldsymbol{\Psi^*}(\boldsymbol{x})$, $\boldsymbol{N^*}(\boldsymbol{x})$, and $\boldsymbol{\sigma_{ij}^*}(\boldsymbol{x})$ are indicates the amplitudes of the field quantities. By using Eq. (33), Eqs. (32)–(35) become:

$$\left(D^2-\zeta_1\right)\Phi^*=\zeta_6\Psi^*+\theta^*+N^*\tag{39}$$

$$\left(D^2-\zeta_2\right)\Psi^*=\zeta_5\Phi^*\tag{40}$$

$$\zeta_7\left(D^2-a^2\right)\Phi^*=\left(D^2-\zeta_3\right)\theta^*+\zeta_8N^*\tag{41}$$

$$\left(D^2-\zeta_4\right)N^*=g_3\theta^*\tag{42}$$

where

$$\zeta_1=\omega^2\left(1+\varepsilon_0\mu_0a_0^2\right)+a^2-\Omega^2,\zeta_2=a^2+\frac{c_0^2\omega^2}{c_3^2}\left(1+\varepsilon_0\mu_0a_0^2\right)-\frac{\Omega^2c_0^2}{c_3^2},$$
$$\zeta_3=a^2+\frac{\omega\left(1+\sum_k^m\frac{\tau_q^{(K\alpha)}}{(K\alpha)!}\omega^{K\alpha}\right)}{\left(1+\sum_{k=1}^{p}\frac{\tau_\theta^{(K\alpha)}}{(K\alpha)!}\omega^{K\alpha}\right)},\zeta_4=a^2+\omega g_1+g_2,\tag{43}$$
$$\zeta_5=\frac{2\Omega c_0^2\omega}{c_3^2},\zeta_6=2\omega\Omega,\zeta_7=\omega\varepsilon_1\left(\frac{1+\sum_k^m\frac{\tau_q^{(K\alpha)}}{(K\alpha)!}\omega^{K\alpha}}{1+\sum_{k=1}^{p}\frac{\tau_\theta^{(K\alpha)}}{(K\alpha)!}\omega^{K\alpha}}\right),\zeta_8=\varepsilon_1\left(\frac{1+\sum_k^m\frac{\tau_q^{(K\alpha)}}{(K\alpha)!}\omega^{K\alpha}}{1+\sum_{k=1}^{p}\frac{\tau_\theta^{(K\alpha)}}{(K\alpha)!}\omega^{K\alpha}}\right).$$

Eliminating $\theta^*(x)$, $\Psi^*(x)$ and $N^*(x)$ in Eqs. (39)–(42), one obtains

$$\left(D^8-AD^6+BD^4-CD^2+E\right)\Phi^*(x)=0\tag{44}$$

with

$$A=\frac{(\zeta_2g_3+\zeta_{14})}{g_3},\quad B=\frac{(\zeta_2\zeta_{14}+\zeta_{15}-\zeta_5\zeta_{12})}{g_3},\quad C=\frac{(\zeta_2\zeta_{15}+\zeta_{16}-\zeta_5\zeta_{12}\zeta_9)}{g_3},E=\frac{(\zeta_2\zeta_{16}-\zeta_5\zeta_{12}\zeta_{10})}{g_3},$$
$$\zeta_{16}=\zeta_1\zeta_{10}g_3+a^2\zeta_{11}\zeta_{13},\zeta_{15}=\zeta_1\zeta_9g_3+\zeta_{11}\zeta_{13}+a^2\zeta_{11}+\zeta_{10}g_3,\zeta_{12}=\zeta_6g_3,$$
$$\zeta_{14}=\zeta_1g_3+\zeta_9g_3,\zeta_{13}=\zeta_4-g_3,\quad\zeta_{11}=\zeta_7g_3,\zeta_{10}=\zeta_8g_3+\zeta_3\zeta_4,\zeta_9=\zeta_3+\zeta_4.\tag{45}$$

Equation (44) can be moderated to

$$\left(D^2-k_1^2\right)\left(D^2-k_2^2\right)\left(D^2-k_3^2\right)\left(D^2-k_4^2\right)\Phi^*(x)=0\tag{46}$$

where k_n^2, $n=1,2,3,4$ are roots of

$$k^8-Ak^6+Bk^4-Ck^2+E=0\tag{47}$$

when Φ^* is bounded at $x\to\infty$, the solution of Eq. (46) is obtained as:

$$\Phi^*(x)=\sum_{n=1}^{4}C_n(a,\omega)e^{-k_nx}\tag{48}$$

In the same manner, we get

$$\left\{N^*,\theta^*,\Psi^*\right\}(x)=\sum_{n=1}^{4}\left\{C_n',C_n'',C_n'''\right\}(a,\omega)e^{-k_nx}\tag{49}$$

Where:

$$C_n'(a,\omega)=H_nC_n(a,\omega),\quad C_n''(a,\omega)=L_nC_n(a,\omega),\quad C_n'''(a,\omega)=M_nC_n(a,\omega)\tag{50}$$

where

$$H_n=\frac{\zeta_{11}\left(k_n^2-a^2\right)}{k_n^4-\zeta_9k_n^2+\zeta_{10}},\quad L_n=\frac{\zeta_{11}H_n\left(k_n^2-\zeta_4\right)}{g_3},\quad M_n=\frac{\zeta_5}{\left(k_n^2-\zeta_4\right)}.\tag{51}$$

Thus, one obtains

$$\left\{N^*,\theta^*,\Psi^*\right\}(x)=\sum_{n=1}^{4}\{H_n,L_n,M_n\}C_ne^{-k_nx}\tag{52}$$

Using the solutions of $\{N^*,\theta^*,\Psi^*\}$ given in Eqs. (49), (52) and (25), we get:

$$u^*(x)=-\sum_{n=1}^{4}(k_n+iaM_n)C_ne^{-k_nx}$$
$$w^*(x)=\sum_{n=1}^{4}(ia-k_nM_n)C_ne^{-k_nx}\tag{53}$$

Substituting Eqs. (49) and (53) into Eqs. (37), in relations of normal modes, we obtain:

$$\sigma_{zz}^*(x)=\sum_{n=1}^{4}R_nC_ne^{-k_nx}$$
$$\sigma_{xz}^*(x)=\sum_{n=1}^{4}Q_nC_ne^{-k_nx}\tag{54}$$

Where

$$R_n=-\left(k_n^2-a^2\right)\left(2\beta^2-1\right)-2ia\beta^2k_nM_n-2a^2\beta^2-L_n-H_n,$$
$$Q_n=2ia\beta^2k_n+a^2\beta^2+\beta^2k_n^2M_n,\quad\beta^2=\frac{c_2^2}{c_1^2}.\tag{55}$$

4 Applications

Now, we will find the parameters C_j, $(j = 1, 2, 3, 4)$. We suppose that the consider half-space is exposed to a normal force on the surface $(x = 0)$ which depends on the time t and the coordinate x such that $(-\infty < x < \infty)$.

On the surface $x = 0$, the boundary conditions are assumed to be [29, 30]:

$$\sigma_{zz}(0,z,t) = -P, \qquad \sigma_{xz}(0,z,t) = 0 \tag{56}$$

$$\left.\frac{\partial\theta(x,z,t)}{\partial x}\right|_{x=0} + h\theta(0,z,t) = 0 \tag{57}$$

$$D_E\left.\frac{\partial N}{\partial x}\right|_{x=0} = s_f N(0,z,t) \tag{58}$$

where s_f is the surface recombination velocity and $h \to 0$ refers to thermally insulated boundaries and $h \to \infty$ denotes the isothermal boundaries.

Substituting the solutions of the σ_{zz}, σ_{xz}, θ and N into the boundary conditions (56)–(58) yields:

$$\sum_{n=1}^{4} R_n C_n = -P\mathrm{e}^{-(\omega t + iaz)} = P_1 \tag{59}$$

$$\sum_{n=1}^{4} Q_n C_n = 0 \tag{60}$$

$$\sum_{n=1}^{4} k_n C_n \mathrm{e}^{-k_n x} = 0 \tag{61}$$

$$\sum_{n=1}^{3} G_n C_n = 0, \quad G_n = L_n\left(D_E k_n + s_f\right) \tag{62}$$

We can put Eqs. (59)–(62) in the following system equation

$$\begin{bmatrix} C_1 \\ C_2 \\ C_3 \\ C_4 \end{bmatrix} = \begin{bmatrix} R_1 & R_2 & R_3 & R_4 \\ Q_1 & Q_2 & Q_3 & Q_4 \\ G_1 & G_2 & G_3 & G_4 \\ k_1H_1 & k_2H_2 & k_3H_3 & k_4H_4 \end{bmatrix}^{-1} \begin{bmatrix} -P_1 \\ 0 \\ 0 \\ 0 \end{bmatrix} \tag{63}$$

Solving the system Eq. (63), we can get the parameters C_j, $j = 1, 2, 3, 4$. Then, we get final expressions for the temperature and displacement distributions, in addition the distributions of other physical quantities.

5 Special Cases

From the governing Eqs. (8), (9), (11) and (12), many of special cases can be obtained, and for example:

- The governing equations of classical photo-thermoelasticity model (CPTE) [55] are be obtained by taking $\tau_q = \tau_\theta = 0$ and $\alpha = 1$.
- The generalized photo-thermoelasticity equations with one relaxation time will be produced (PLS) [56] by setting $\tau_\theta = 0,\ \tau_q > 0,\ \alpha = 1$ and $m = 1$.
- The equations of generalized photo-thermoelasticity involve thermal lagging in the form of dual-phase-lags (PDPL) result by letting $\tau_\theta > 0,\ \tau_q > 0,\ \alpha = 1,\ m = 2$ and $p = 1$.
- The equations of generalized model of photo-thermoelasticity of higher-order time-derivatives with dual-phase-lags (HPDPL) are determined by letting $\tau_\theta > 0,\ \tau_q > 0,\ \alpha = 1,\ m \geq 2$ and $p \geq 1$.
- The equations of the classical fractional photo-thermoelasticity model (FCPTE) result by letting $\tau_q = \tau_\theta = 0$ and $0 < \alpha \leq 1$.
- The model of generalized fractional photo-thermoelasticity with one relaxation time result (FPLS) [57] by letting $\tau_\theta = 0,\ \tau_q > 0,\ 0 < \alpha \leq 1$ and $m = 1$.
- The equations of fractional photothermoelasticity with dual-phase-lags proposed by Ezzat [58] (FEPTE) result by letting $\tau_\theta > 0,\ \tau_q > 0,\ 0 < \alpha \leq 1,\ m = 2$ and $p = 1$.
- The equations of generalized model of fractional photothermoelasticity of higher-order time-derivatives with dual-phase-lags introduced by Abouelregal (HADPL) [40] result by letting $\tau_\theta = 0,\ \tau_q > 0,\ \alpha = 1,\ m \geq 2,\ 0 < \alpha \leq 1$ and $p \geq 1$.

6 Numerical Applications

The validity of the proposed model is investigated via introducing some numerical computations. For this objective, the values of the involved physical parameters for magnesium (Mg) are [59, 60]:

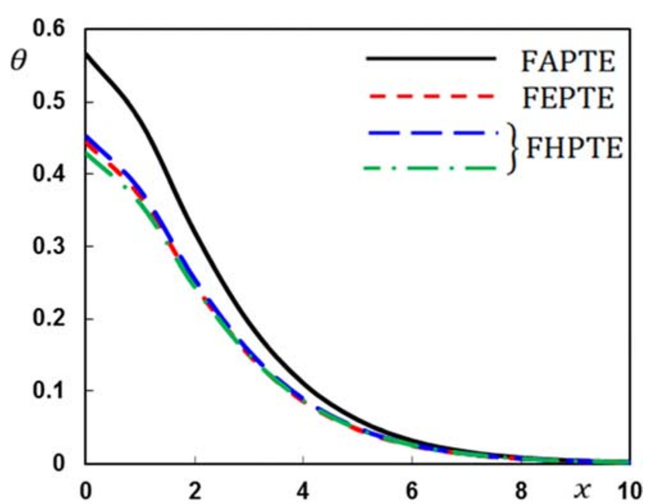

Fig. 1 The distribution of temperature θ with the higher order parameters m, p

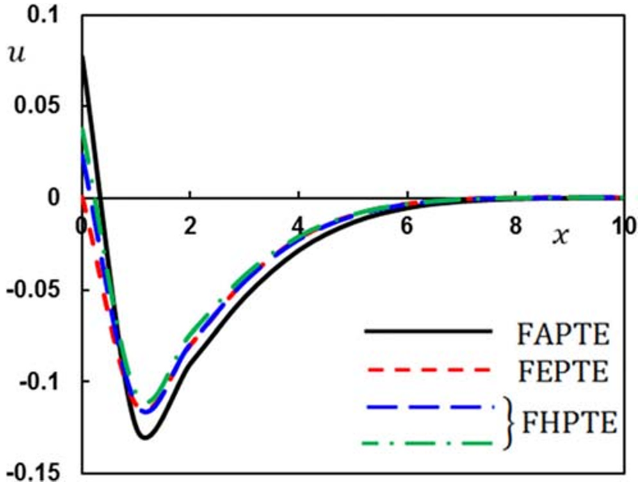

Fig. 2 The distribution of displacement u with higher order parameters m, p

$$\lambda = 2.696 \times 10^{10}\text{kg m}^{-1}\text{s}^{-2},\quad \mu = 1.639 \times 10^{10}\text{kg m}^{-1}\text{s}^{-2},\quad \rho = 1740\ \text{kg m}^{-3},$$
$$K = 2.510\ \text{W m}^{-1}\text{K}^{-1},\quad C_E = 1.04 \times 10^{3}\ \text{J kg K}^{-1},\quad d_n = -9 \times 10^{-31}\ \text{m}^3,$$
$$E_g = 1.11\ \text{eV},\quad D_E = 2.5 \times 10^{-3}\ \text{m}^2\ \text{s}^{-1}, s_f = 2\ \text{m s}^{-1}, \tau = 5 \times 10^{-5}\ \text{s}, T_0 = 298\text{K}.$$

The other magnetic constants are taken as

$$\varepsilon_0 = \frac{10^{-9}}{36\pi}\ \text{Fm}^{-1},\quad \mu_0 = 4\pi \times 10^{-7}\ \text{Hm}^{-1}, H_0 = \frac{10^7}{4\pi}\ \text{Am}^{-1}.$$

Since ω is complex ($\omega = \omega_0 + i\omega_1$), we can take $\omega_0 = 0.1$ and $\omega_1 = 1$. Also, the computations are obtained for small value of the time $t = 0.1$s and $h \to 0$. The real part of both temperature distribution θ, normal displacement u, normal stress σ_{zz}, tangential stress σ_{xz}, and carrier charge density N with distance x at the plane $z = 1$. The variants of the studied field variables are plotted in Figs. 1, 2, 3, 4, 5, 6, 7 ,8 ,9, 10, 11, 12, 13, 14 and 15.

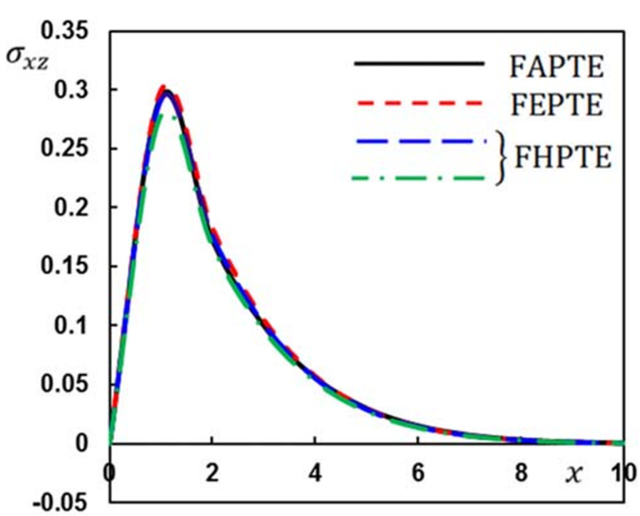

Fig. 3 The distribution of stress σ_{xz} with higher order parameters m, p

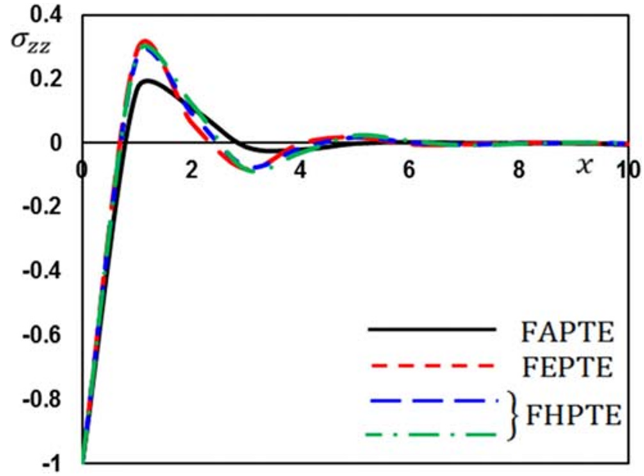

Fig. 4 The distribution of stress σ_{zz} with higher order parameters m, p

Comparisons of these physical fields are committed to three different categories.

6.1 Comparison of Different Models of Fractional Photo-Thermoelasticity

In this case, the influence of higher-order time fractional parameters p and m = $p + 1$ will be investigated. Also the distributions corresponding to unified new model (**FHPTE**) are compared with Ezzat (**FEPTE**) and Abouelregal (**FAPTE**) models. The obtained results for the field quantities for various high orders m and p are depicted in Figs. 1, 2, 3, 4, and 5 with horizontal distance x. Other physical parameters remain constants ($\alpha = 0.7$, $\tau_\theta = 0.05$, $\tau_\theta = 0.1$ and $\Omega = 0.3$). It is evident in all plots that, inside the medium, the thermal waves are propagated with faster and finite, according to the higher-order fractional derivative values. Thus, it is necessary to take into consideration p values until the material reaches a stable state.

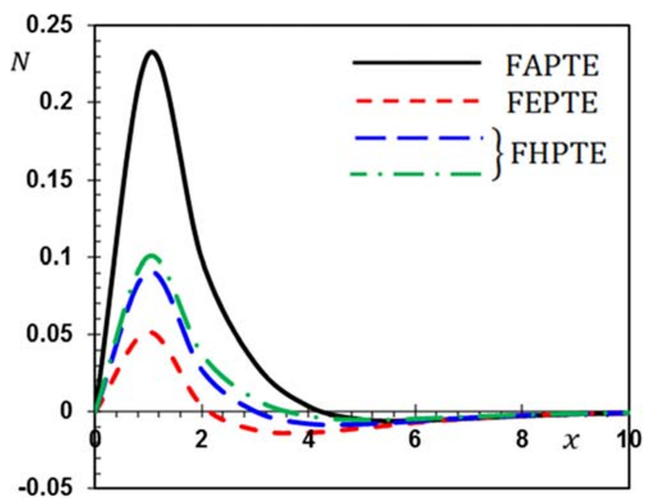

Fig. 5 The distribution of carrier charge density N with higher order parameters m, p

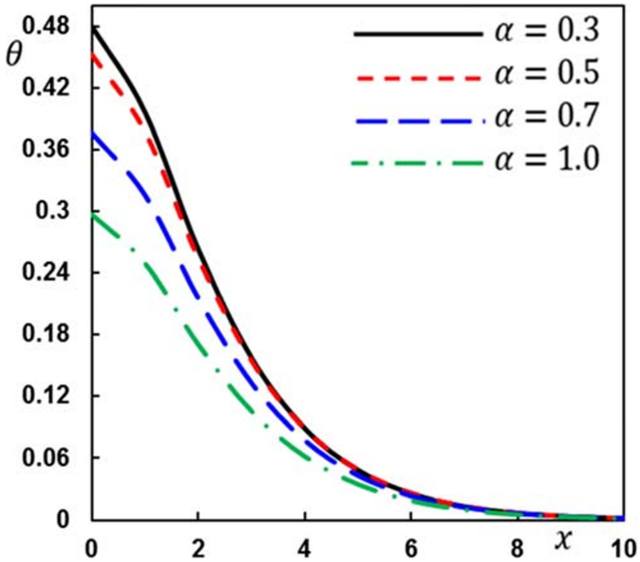

Fig. 6 The distribution of temperature θ with fractional order parameter α

As indicated in Fig. 1 **FHPTE** model represents the smallest temperature values while the highest values are reached by the **FEPTE** model. Figure 4 clearly show that normal stress σ_{zz} starts with negative value at the distance $x = 0$ and increases rapidly with the increases of x –values until it approaches zero for all the different models.

- The distributions of all studied physical quantities tends to zero when the distance x attend to infinity.
- Changes of the temperature θ starts with the largest values on the boundary of medium and progressively decreases in direction of vanishing with x.
- Also, as shown in Fig. 2, the normal displacement distribution, in the three models approximately behaves the same.

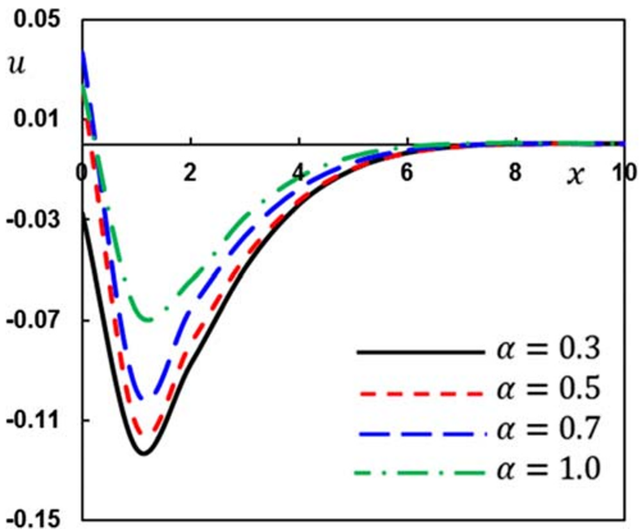

Fig. 7 The distribution of displacement u with fractional order parameter α

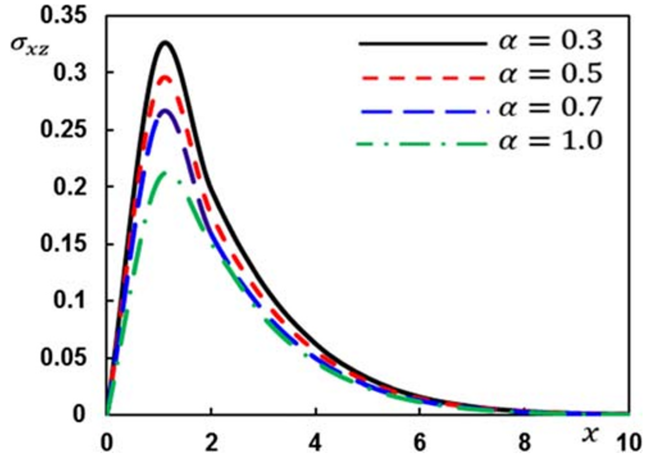

Fig. 8 The distribution of the stress σ_{xz} with fractional order parameter α

- The thermal stress σ_{zz} have Synchronized starting point for all the three models, it starts with the value $\sigma_{zz} = -P = -1$ at $x = 0$ which verifies that it satisfies the surface condition at the boundary $x = 0$.
- The thermal stress σ_{xz} maximum values occur at $x = 1$, then it decreases and finally fades away identically as x increases for all the three models. Its profile is compressive in nature close to the surface $x = 0$ and with the increase of x, it decreases to zero value which is absolutely acceptable.
- Except the stress σ_{xz}, all distributions have non-zero values only in surface area of the body. Outside this area, the distributions vanishes typically which be in conformity with the experimental results. This demonstrates that, a design depend on hyperbolic heat conduction model is a greater amount physically sensible over that depend on Fourier law of heat conduction.
- The carrier density N increases at the beginning and starts decreasing at $x = 1$ (maximum) and finally converges to zero values as x increases.

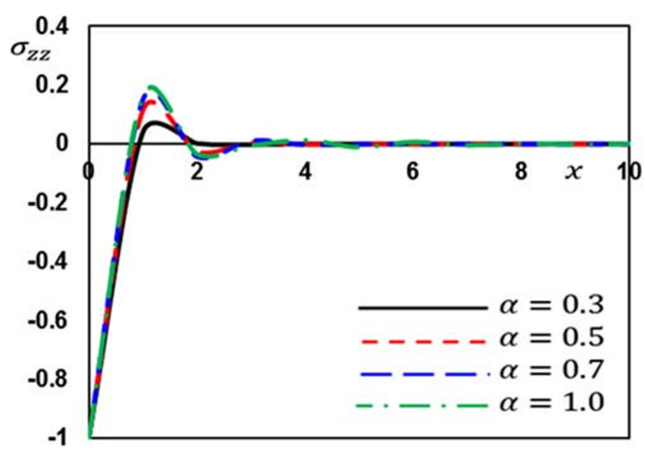

Fig. 9 The distribution of the stress σ_{zz} with fractional order parameter α

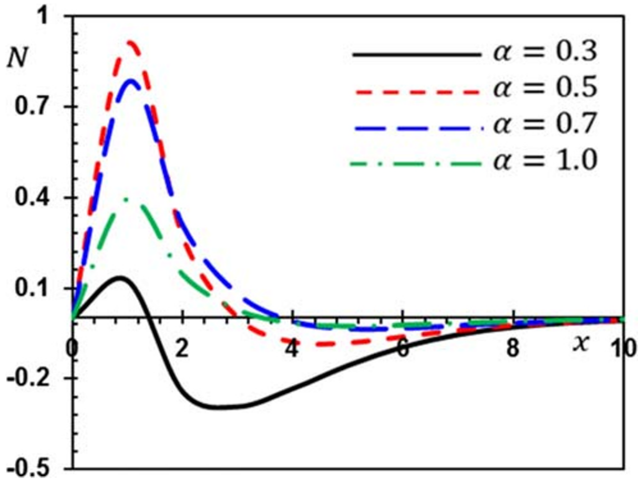

Fig. 10 The distribution of carrier density N with fractional order parameter α

- The **FEPTE** model with ($m = 1$) gives the largest values of thermal stresses at $\alpha = 0.7$ while the smallest values of thermal stresses is given by **FHPTE** model with ($m = 5$) .
- The outcomes in Abouelregal fractional photo-thermoelasticity modified model (**FAPTE**) are different by comparing it with the other models (**FEPTE** and **FHPTE**).
- The mechanical distributions indicate that the thermoelastic waves propagate with finite velocity in the medium.
- Figures 1, 2, 3,4, 5 display the vibration of the normal displacement and the other field functions with x for the models. Inspection of these diagrams shows that the results of these three fractional models are compatible.

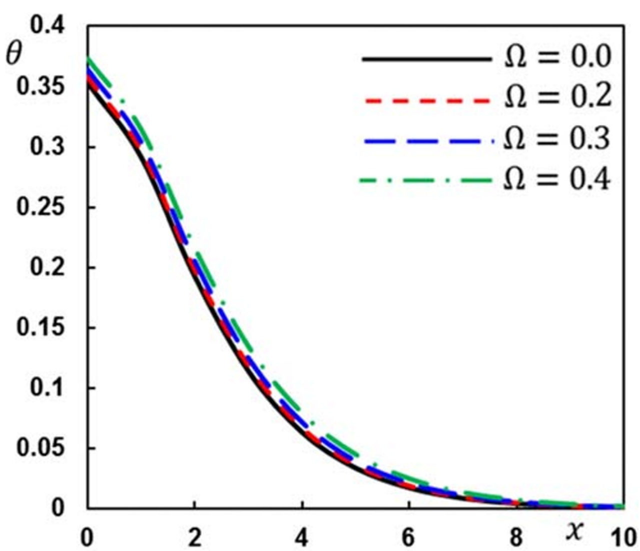

Fig. 11 The distribution of temperature θ with distance x for various values of rotation Ω

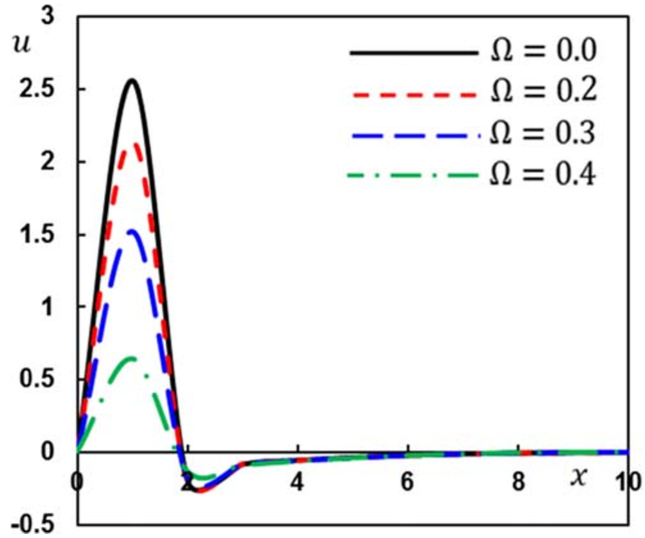

Fig. 12 The distribution of displacement u with distance x for various values of rotation Ω

- The new model of Abouelregal is in finite similar to the other models and agrees with the physical behaviors of thermoelastic materials.

6.2 Influence of the Fractional Order Parameter

This case represent the variations of normal displacement u, normal force stress σ_{zz}, tangential stress σ_{xz}, temperature distribution θ and carrier charge density N for varying values of fractional order derivative ($0 < \alpha \leq 1$) when $\Omega = 0.3$, $\tau_\theta = 0.05$, $\tau_\theta = 0.1$ and $p = 3$.

It is noticed that when $\alpha = 1.0$ refers to normal conductivity (without-fractional) and when $0 < \alpha < 1$ refers to the weak

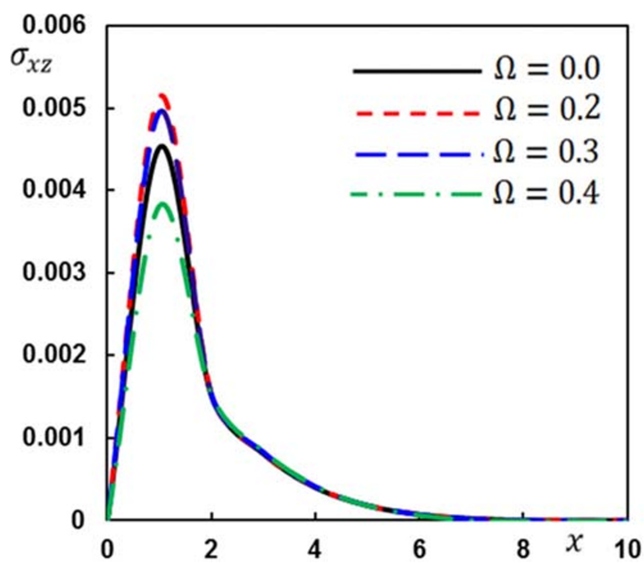

Fig. 13 The distribution of the tangent stress σ_{xz}w with distance x for various values of rotation Ω

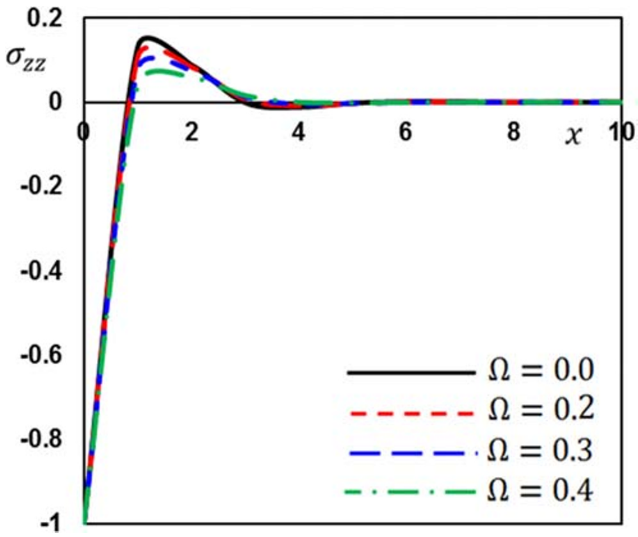

Fig. 14 The distribution of the normal stress σ_{zz} with distance x for various values of rotation Ω

conductivity (fractional). The effect of the fractional order parameter on all studied distributions is shown in Figs. 6, 7, 8, 9, and 10. As shown in all figures, the points in the curved lines indicate how the different fields change with the fractional order parameter.

From the figures we found that:

- Temperature field starts with positive values and its peak values comes near the surface boundary, for the four cases ($\alpha = 1$, $\alpha = 0.7$ and $\alpha = 0.5$, $\alpha = 0.3$), which investigates the effect of fractional derivative and with the increase of x, θ diminishes to zero value which is quite plausible (see Fig. 6), so we can say the fractional derivative have remarkable effects on the temperature field profile.

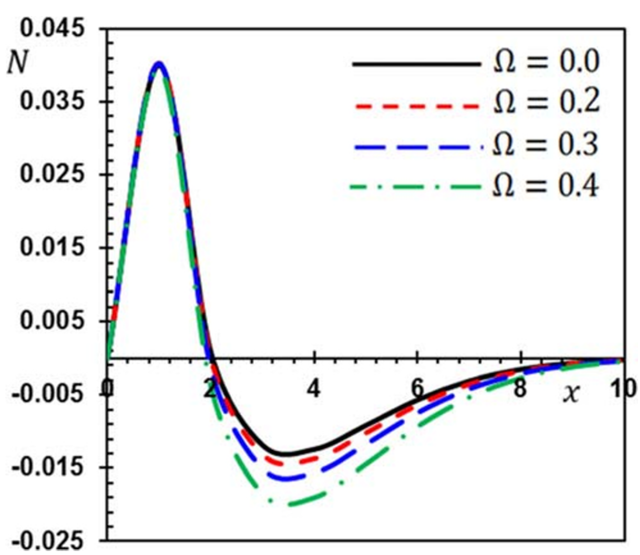

Fig. 15 The distribution of carrier density N $\sigma_{xz}$with distance x for various values of rotation Ω

- It is evident that the parameter α acts to decrease the distribution of temperature field and increase the amplitudes of the normal displacement u and the stress σ_{zz} and has a respectable effect on the carrier density N.
- Time for temperature to arrive to steady state case is nearly similar for every value of α.
- From Fig. 7, it is clear that, under effect of fractional derivative, there is increasing with decreasing values of the fractional parameter α.
- Figures 9 show that the distribution of stress σ_{zz} when $\alpha = 0.7$ is higher than the values in the case $\alpha = 0.5, 0.3$ which investigates that the fractional parameter is having an increasing Influence on stress field σ_{zz}.
- According to our results, which consistent with the numerical results given in [56], we need to develop a new classification to every one of the materials as per their fractional coefficient, where this parameter turns out to be new pointer of its capacity to conduct the thermal energy.

6.3 Influence of the Rotation

When the medium is rotating with an angular velocity Ω, we established the centripetal acceleration and Coriolis increasing speed as a two further terms in the equation of motion, which effects the thermoelastic response. In this case, we take into consideration four values of the parameter of rotation $\Omega = 0$, $\Omega = 0.2$, $\Omega = 0.3$ and $\Omega = 0.4$, while the other parameters have been taken as $z = 1$, $\tau = 0.002$, and the parameter $\alpha = 0.7$.

Figures 11, 12, 13, 14 and 15 are sketched to introduce a comparison between the obtained results for normal displacement u, normal force stress σ_{zz}, tangential stress σ_{xz}, temperature distribution θ and carrier charge density N against positions x in cases of nonappearance and presence of the rotation parameter Ω.

From all these figures, it is evident that:

- All curves Synchronized when x tends to infinity and all physical distribution fields satisfy the boundary conditions.
- The rotating field has noticeable effects on all the profiles of the studied fields.
- The rotation parameter Ω acts to decrease the non-dimensional displacement u,the stress σ_{xz}, normal stress σ_{zz}. and the carrier charge density field N whereas acts to increase temperature distribution θ.

7 Conclusions

In this work, a new model for photo-thermoelasticity with fractional higher-order time and phase lags (**FAPTE**) is constructed. To study the accuracy and validity of the introduced model, a two dimensional problem in a rotating semiconductor medium subjected to mechanical force and magnetic field is investigated. The effects of higher-order time-fractional, fractional and rotation parameters on the resulting fields have been discussed and depicted graphically. From the present investigation several interesting particular cases are deduced.

From the theoretical and numerical results, we can observe and conclude that all the studied fields are significantly dependent on the higher-order time-fractional derivatives and fractional parameters. The studied variables reach a steady state based on the choice of the higher-order time-fractional values.

This work also suggests that, the modified model with higher-order time-fractional (**FAPTE**) explains the response of the thermoelastic materials more realistically than the classical model of photo-thermoelasticity. In addition, our results can be useful to researchers for investigation and design of the thermal, plasma and a beat laser covered materials, as well as several engineering performs related to boundary investigation and design.

References

1. Oldham KB, Spanier J (1974) The fractional calculus: theory and application of differentiation and integration to arbitrary order. Academic Press, New York
2. Samko SG, Kilbas AA, Marichev OI (1993) Fractional integrals and derivatives: theory and applications. Gordon and Breach Science Publishers, London
3. Miller KS, Ross B (1993) An introduction to the fractional calculus and fractional differential equations. Wiley, New York
4. Podlubny I Fractional differential equations. Academic Press, New York (1999)
5. Povstenko YZ (2005) Fractional heat conduction equation and associated thermal stress. J Therm Stresses 28:83–102
6. Caputo M (1967) Linear model of dissipation whose Q is almost frequency independent-II. Geophys J R Astron Soc 13:529–539
7. Abd El-Latief AM (2016) Application of generalized fractional thermoelasticity theory with two relaxation times to an electromagnetothermoelastic thick plate. Adv Mater Sci Eng 2016:5821604. https://doi.org/10.1155/2016/5821604
8. Sherief HH, El-Sayed A, El-Latief AM (2010) Fractional order theory of thermoelasticity. Int J Solids Struct 47:269–275
9. Abouelregal AE (2011) Fractional order generalized thermo-piezoelectric semi-infinite medium with temperature-dependent properties subjected to a ramp-type heating. J Therm Stresses 34(11):1139–1155
10. Abouelregal AE, Zenkour AM (2013) The effect of fractional thermoelasticity on a two-dimensional problem of a mode I crack in a rotating fiber-reinforced thermoelastic medium. Chin Phys B 22(10):102–108
11. Abouelregal AE (2016) Fractional heat conduction equation for an infinitely generalized, thermoelastic, long solid cylinder, international. J Comput Meth Eng Sci and Mech 17(5–6):374–381
12. Zenkour AM, Abouelregal AE (2014) State-space approach for an infinite medium with a spherical cavity based upon two-temperature generalized thermoelasticity theory and fractional heat conduction. Z Angew Math Phys 65(1):149–164
13. Lord H, Shulman Y (1967) A generalized dynamical theory of thermoelasticity. J Mech Phys Solid 15:299–309
14. Green AE, Naghdi PM (1993) Thermoelasticity without energy dissipation. J Elast 31:189–209
15. Sharma JN, Othman MIA (2007) Effect of rotation on generalized thermo-viscoelastic Rayleigh-lamb waves. Int J Solids Struct 44: 4243–4255
16. Sharma JN, Thakur MD (2006) Effect of rotation on Rayleigh-lamb waves in magneto-thermoelastic media. J Sound Vib 296(4–5): 871–887
17. Othmanand MIA, Song YQ (2008) Reflection of magneto-thermoelastic waves from a rotating elastic half–space. Int J Eng Sci 46(5):459–474
18. Othman MIA, Zidan MEM, Hilal MI (2013) Influence of gravitational field and rotation on thermoelastic solid with voids under green-naghdi theory. J Phys 2:22–34
19. Dovichi NJ, (1987) CRC critical reviews in analytical chemistry 17 357
20. Tam, A. C. in Ultrasensitive laser spectroscopy kliger, D. S., Editor, Academic Press, New York (1983)
21. Tam AC (1985) Pulsed photothermal radiometry for noncontact spectroscopy, material testing and inspection measurements. Infrared Physics 25(1):305–313
22. Tam AC (1986) Applications of photoacoustic sensing techniques. Rev Mod Phys 58:381–431
23. Sell JA (1989) Photothermal investigations in solids and fluids. Academic Press, Inc. New York
24. Bell AG (1880) On the production and reproduction of sound by light. Am J Sci, Series 3(20):305–324
25. Bell AG (1881) Upon the production of sound by radiant energy. Philos Mag Series 5 11(71):510–528
26. Viengerov ML (1938). Dokl Akad Nauk SSSR 19:687
27. Rosencwaig A, Opsal J, Willenborg DL (1983) Thin-film thickness measurements with thermal waves. Appl Phys Lett 43(2):166–168
28. Song Y, Todorovic DM, Cretin B, Vairac P (2010) Study on the generalized thermoelastic vibration of the optically excited semiconducting microcantilevers. Int J Solids Struct 47(14):1871–1875
29. Song Y, Todorovic DM, Cretin B, Vairac P, Xu J, Bai J (2014) Bending of semiconducting cantilevers under photothermal excitation. Int J Thermophys 35(2):305–319
30. Todorovic DM (2003) Plasma, thermal, and elastic waves in semiconductors. Rev Sci Instrum 74:582
31. Mondal S, Sur A (2020) Photo-thermo-elastic wave propagation in an orthotropic semiconductor with a spherical cavity and memory responses. Waves Random Complex Media. https://doi.org/10.1080/17455030.2019.1705426
32. Mondal S, Sur A, Kanoria M (2019) Photo-thermo-elastic wave propagation under the influence of magnetic field in presence of memory responses. Mech Based Design Struct Mach. https://doi.org/10.1080/15397734.2019.1701493
33. Sarkar N, Mondal S (2019) Thermoelastic interactions in a slim strip due to a moving heat source under dual-phase-lag heat transfer. J Heat Transf 141(12):124501 HT-19-1157
34. Mondal S (2019) Memory response in a magneto-thermoelastic rod with moving heat source based on eringen's nonlocal theory under dual-phase lag heat conduction. Int J Comput Methods. https://doi.org/10.1142/S0219876219500725
35. Mondal S, Sarkar N, Sarkar N (2019) Waves in dual-phase-lag thermoelastic materials with voids based on Eringen's nonlocal elasticity. J Therm Stresses 42(8):1035–1050. https://doi.org/10.1080/01495739.2019.1591249
36. Elsherbeny KZ, Abouelregal AE, Abo-Dahab SM, Rashid AF (2016) Thermoelastic analysis for an infinite solid cylinder due to

harmonically varying heat with thermal conductivity variable. J Comput Theor Nanosci 13(7):4493–4500
37. Abouelregal AE (2020) Modified fractional photo-thermoelastic model for a rotating semiconductor half-space subjected to a magnetic field. Silicon. https://doi.org/10.1007/s12633-020-00380-x
38. Chirita S, Zampoli V (2018) Spatial behavior of the dual-phase-lag deformable conductors. J Thermal Stress 41(10–12):1276–1296
39. Chirita S (2019) On high-order approximations for describing the lagging behavior of heat conduction. Math Mech Solids 24(6): 1648–1667
40. Abouelregal AE (2019) Modified fractional thermoelasticity model with multi-relaxation times of higher order: application to spherical cavity exposed to a harmonic varying heat. Waves Random Complex Media 17(1):1745–5030
41. Green AE, Lindsay KA (1972) Thermoelasticity. J Elast 2(1):1–7
42. Abouelregal AE, (2019) Two-temperature thermoelastic model without energy dissipation including higher order time-derivatives and two phase-lags, mater Res Express 6 116535, https://doi.org/10.1088/2053-1591/ab447f
43. Abouelregal AE (2019) On Green and Naghdi thermoelasticity model without energy dissipation with higher order time differential and phase-lags. J Appl Comput Mech 6(3):445–456
44. Quintanilla R (2008) A well-posed problem for the dual-phase-lag heat conduction. J Therm Stresses 31:260–269
45. Majchrzak E (2010) Numerical solution of dual phase lag model of bioheat transfer using the general boundary element method. CMES 69(1):43–60
46. Rukolaine SA (2017) Unphysical effects of the dual-phase-lag model of heat conduction: higher-order approximations. Int J Therm Sci 113:83–88
47. Tzou DY (1995) Experimental support for the lagging behavior in heat propagation. J Thermophys Heat Transf 9:686–693
48. Tzou DY (1996) Macro-to-microscale heat transfer: the lagging behavior. Washington, DC, Taylor & Francis
49. Jumarie G (2010) Derivation and solutions of some fractional black-Scholes equations in coarsegrained space and time. Application to Merton's optimal portfolio. Comput Math Appl 59:1142–1164
50. Carpinteri A, Mainardi F (1997) Fractals and fractional calculus in continuum mechanics. Springer, New York (NY)
51. Povstenko YZ (2009) Thermoelasticity that uses fractional heat conduction equation. J Math Sci 162(2):296–305
52. Biswas P, Singh S and Bindra H, (2019) A closed form solution of dual phase lag heat conduction problem with time periodic boundary conditions, journal of heat transfer, ASME, 1:paper # HT-18-1429
53. Rafiq M, Singh B, Arifa S, Nazeer M, Usman M, Arif S, Bibi M, Jahangir A (2019) Harmonic waves solution in dual-phase-lag magneto-thermoelasticity. Open Phys 17:8–15
54. Sharma JN, Walia V (2007) Effect of rotation on Rayleigh waves in piezothermoelastic half space. Int J Solids Struct 44(3–4):1060–1072
55. Song ZYQ, Bai JT, Ren Y (2012) Study on the reflection of photothermal waves in a semiconducting medium under generalized thermoelastic theory. Acta Mech 223:1545–1557
56. Abbas I, Alzahrani F, Berto F (2018) The effect of fractional derivative on photo-thermoelastic interaction in an infinite semiconducting medium with a cylindrical hole. Engineering Solid Mechanics 6(3):275–284
57. Hobiny A, Abbas I (2018) Analytical solution of fractional order photo-thermoelasticity in a non-homogenous semiconductor medium. Multidiscip Model Mater Struct. https://doi.org/10.1108/MMMS-11-2017-0137
58. Ezzat MA (2011) Theory of fractional order in generalized thermoelectric MHD. Appl Math Model 35:4965–4978
59. Dhaliwal RS, Singh A (1980) Dynamical coupled thermoelasticity. Hindustan Publishers, Delhi
60. Ailawalia P, Kumar A (2019) Ramp type heating in a semiconductor medium under photothermal theory. Silicon. https://doi.org/10.1007/s12633-019-00130-8